Available online at www.sciencedirect.com
ScienceDirect
International Journal of Sediment Research 29 (2014) 378-390
INTERNATIONAL JOURNAL OF SEDIMENT RESEARCH
www.elsevier.com/locate/ijsrc

Experimental modelling of flocculation processes-the case of Paraiba do Sul Estuary

Alfredo TRENTO[1] and Susana VINZÓN[2]

Abstract

The aggregation dynamics of fine sediments was analysed through laboratory tests using Couette and disk flocculators. It was shown that floc sizes tend to increase as concentrations grow both in fresh and salt water, in agreement with the aggregation theory, and that equilibrium diameters are slightly greater in salt environments for flocs developed either under shear stress or by differential sedimentation. Their transport and the aggregation processes were preliminarily studied in the estuary of the Paraíba do Sul River using a particle tracking model and field data. The floc breakup process by shear stress was included in the model. Yield stresses, which were determined by fractal dimensions and differential density, were accounted for. After the calibration of the collision efficiency coefficients, the numerical model was able to predict floc sizes comparable with those measured at the Paraíba do Sul estuary, which, in turn, were similar to those obtained during the laboratory experiments in the Couette flocculator.

Key Words: Flocs, Flocculators, Transport processes, Paraíba do Sul

1 Introduction

The characterization of fine suspended sediment transport and flocculation in estuaries has environmental implications as these aggregates can catch both organic and inorganic matter (Edszwald et al., 1974; Gibbs, 1983; Droppo et al., 2005). In order to understand the dynamics of flocculation it is necessary to comprehend the interaction of many physico-chemical processes that favor the aggregation of cohesive particles; and on the other hand, the endless process of floc growth and breakup, as well as the complex dynamics of advection-dispersion that applies to estuaries. These difficulties appear when trying to find a mathematical representation for the phenomenon or a numerical approximation to the differential equations. The aggregation process is controlled by a combination of hydrodynamic and surface-chemical interactions. The aggregation of particles in the aqueous systems occurs by Brownian diffusion, turbulent shear flow, or differential settling (Walker and Bob, 2001; Kim and Stolzenbach, 2004). Current shear, expressed in terms of fluid shear rate, is typically the most important factor contributing to aggregation in turbulent flows. These processes are nonlinear, and this leads to difficulties in the mathematical theory (Friedlander, 2000).

Laboratory experiments allow the study of the complex process of flocculation under controlled conditions, where each of the basic process can be observed. For instance, flocculation in settling columns was analised by Farley and Morel (1986), Torfs et al. (1996), Johansen and Larsen (1998), Milligan and Hills (1998), Curran et al. (2003); in annular flumes by Mehta and Partheniades (1975), Lau and Krishnappan (1992), Manning and Dyer (1999), Yang et al. (2000), Manning et al. (2007); in Couette devices by van Duuren (1968), Ives and Bohle (1973), Hunt (1982), Gibbs (1983), Tsai et al. (1987), Serra and Casamitjana (1998), Neumann (2004), Serra et al. (2008); in jars by Ives and Bohle (1977), Mikes et al. (2004), Coufort et al. (2005), Cheng et al. (2008), Kumar et al. (2010) ; and in disk devices by Tooby et al. (1977), Lick et al. (1993), Jackson (1994), Huang (1994), among others.

The reported experiments were relevant for the scientific community because they showed how to obtain the main variables of flocculation processes studied, either by direct or indirect measurement in some cases, or by calculating the parameters of aggregation and disaggregation in others or process simulation. The contribution aimed in this paper is to integrate independent results from field and laboratory flocculation experiments and the numerical simulations of sediment transport in a natural estuary scenario. Thus, flocculation laboratory experiments are reported, aiming to determine the relevant parameters of the flocculation process. A sediment transport numerical model was developed and applied to Paraíba do Sul estuary (Brazil). In this model, the flocculation sub-model was based on the algorithm

[1] Prof. Dr., Department of Hydraulics, National University of Litoral, Santa Fe, Argentina. E-mail: alfredotrento@yahoo.com.
[2] Prof. Dr., Programa de Engenharia Oceânica (PEnO)/COPPE, Federal University of Rio de Janeiro, Rio de Janeiro, Brazil. E-mail: susanavinzon@gmail.com
Note: The original manuscript of this paper was received in Dec. 2012. The revised version was received in Mar. 2014. Discussion open until Sept. 2015.

proposed by Farley and Morel (1986). This algorithm was already applied by Hayter and Pakala (1989) and Burd et al. (2000). The model results are compared with field measurements carried out in the estuary in January 2004.

2 Sediment transport model

The mathematical model for calculating the fine sediment transport is based on the two-dimensional depth integrated advection-dispersion equation.

$$\frac{\partial C}{\partial t}+\frac{\partial UC}{\partial x}+\frac{\partial VC}{\partial y}=\frac{1}{h}\frac{\partial}{\partial x}\left(h\,D_{xx}\frac{\partial C}{\partial x}\right)+\frac{1}{h}\frac{\partial}{\partial y}\left(h\,D_{yy}\frac{\partial C}{\partial y}\right)+\frac{1}{h}\left(m_e-m_s\right) \tag{1}$$

where C is the mean concentration in the vertical profile; U and V, vertical mean velocities; h is the depth; D_{xx} and D_{yy} are dispersion coefficients for the x and y horizontal orthogonal axes, respectively; and t is time. The erosion rate, m_e, was defined using the Ariathurai and Arulanandan equation (1978) where the main parameter is the critical shear stress for erosion, τ_e. The deposition rate, m_d, was calculated as suggested by Nicholas et al. (2006),

$$m_d=C\left\{\lambda\,W_s\left[1-\left(\hat{U}/U_{cr}\right)^2\right]+q\,p\,E\right\} \tag{2}$$

U_{cr}, is the critical mean flow velocity for sedimentation, $\hat{U}=(U^2+V^2)^{0.5}$ is speed vector module, W_s is the floc vertical mean settling velocity, λ is a calibration parameter, q is floodplain unit flow, p is proportion of the water column occuppied by vegetation and E is vegetation trapping efficiency per unit distance. If there is no floodplain flow, then q = 0. The numerical model used for solving the transport Eq. (1) uses a Lagrangian numerical scheme, Random Walk Particle Tracking (RWPT) model (Dimou and Adams, 1993). The theory of particle trajectory method is based on the analogy between the Fokker-Planck equation and the advection-diffusion equation (Jin, 1993). According to the method, the position of each particle in a rectangular coordinate system is represented by the vector $X(t)$. Random motion of each particle is described by a nonlinear equation of Langevin (Dimou and Adams, 1993):

$$\frac{dX}{dt}=A(X,t)+B(X,t)\,\xi(t) \tag{3}$$

in which $A(x, t)$ is a vector representing the deterministic component, the variable $B(X, t)$ is a tensor that characterizes the random component, and $\xi(t)$ is a vector composed of random numbers. Then, by analogy, it can be obtained for the two dimensional equations:

$$\Delta x=\left(U+\frac{D_{xx}}{h}\frac{\partial h}{\partial x}+\frac{\partial D_{xx}}{\partial x}\right)\Delta t+Z_1\sqrt{2\,D_{xx}\Delta t} \tag{4}$$

$$\Delta y=\left(V+\frac{D_{yy}}{h}\frac{\partial h}{\partial y}+\frac{\partial D_{yy}}{\partial y}\right)\Delta t+Z_2\sqrt{2\,D_{yy}\Delta t} \tag{5}$$

where Z_1 and Z_2 are independent random numbers. The first term on the right represents the deterministic displacement and the second term, the random displacement. The deterministic term has three components: the mean flow velocities, bathymetric gradients and gradients last scattering coefficients due to non-homogeneity of the coefficients.

In order to calculate W_s the Farley and Morel (1986) algorithm was considered, which takes into account the different flocculation mechanisms, Brownian motion, differential sedimentation and shear stresses. This algorithm adopts the assumption that all sediments are flocculated.

$$W_s=\left(-B_{ds}C^{2.3}-B_{sh}C^{1.9}-B_bC^{1.3}\right)/\frac{\partial c}{\partial z} \tag{6}$$

$\partial c/\partial z$ is the vertical sediment concentration gradient, for the vertically integrated model was parametrized as C/h. B_b, B_{ds}, B_{sh} are functional relationships representing each flocculation mechanism given by

$$B_b=1.33(S/h)^{0.6}\rho_f^{-0.3}(\alpha_bK_b)^{0.4} \tag{7.a}$$

$$B_{ds}=3.12(S/h)^{-0.32}\rho_f^{-1.3}(\alpha_bK_b)^{0.17}(\alpha_{ds}K_{ds})^{1.15} \tag{7.b}$$

$$B_{sh}=10(S/h)^{0.15}\rho_f^{-0.9}(\alpha_bK_b)^{0.1}(\alpha_{sh}K_{sh})^{0.75} \tag{7.c}$$

The Farley & Morel algorithm adopts the assumption that the Brownian flocculation can coexist with the flocculation process by differential sedimentation, Eq. (7.b), or with the flocculation process due to shear stresses, Eq. (7.c), where

$$S/h=\left(1/6\pi^2\right)\left(g/3\upsilon h\right)\Delta\rho_f/\rho_w \tag{8}$$

in Eq. 7, S/h is a dimensional parameter for Stokes settling, where $\Delta\rho_f=\rho_f-\rho_w$ is the floc differential density.

$$K_b=2kT/(3\mu) \tag{9.a}$$

$$K_{ds}=(6/\pi)^{1/3}g/(12\upsilon)(\rho_f-\rho_w)/\rho_w \tag{9.b}$$

$$K_{sh}=G/\pi \tag{9.c}$$

K_b, K_{ds} and K_{sh} are dimensional parameters for the collision frequency functions for Brownian motion, differential settling and fluid shear, respectively. g is the gravitational acceleration, T is the absolute temperature, k is the Boltzmann constant, μ and υ are the dynamic and kinematic viscosities of the fluid, respectively, ρ_f is the floc density, ρ_w is the

water density, G is the shearing rate or dissipation parameter, α_b, α_{ds} and α_{sh} are collision efficiency parameters for Brownian motion, differential sedimentation and fluid shear, respectively. Following the work by Kim and Stolzenbach (2004), where the differential settling collision efficiency was evaluated, α_{ds}=0.01 was arbitrated. The Brownian motion was demonstrated irrelevant for particles bigger than 1 μm, then the model results were not sensible to the collision efficiency. A value of α_b=0.1 was considered for all the simulations. A mean value for the collision efficiency by shear stress α_{sh}=0.08 is estimated from the laboratory data presented in section 3.1 and theoretical consideration made by Edzwald et al. (1974), which gives

$$\alpha_{sh} = -\left(\pi \rho_s / 4GT_e C\right) \Delta\rho_f \Big/ \left(\rho_s - \rho_w\right) \ln\left[\rho_s / \rho_f \left(d_p / d_f\right)^3\right] \tag{10}$$

where T_e is the equilibrium time and ρ_s is the sediment density. Edzwald et al. (1974) obtained $0.018<\alpha_{sh}<0.148$, using samples from Pamlico estuary; Gibbs (1983) obtained α_{sh} =0.69, α_{sh} =0.23 and α_{sh} =0.077, for samples obtained from the Amazon, Yukon and Delaware Rivers, using a Couette device and a paddle reactor, and Logan and Kilps (1995) obtained $0.0023< \alpha_{sh}<0.24$ with a paddle flocculator. McAnally and Mehta (2002) proposed an equation based on salinity, temperature, aggregate size, cation exchange capacity, shear stress, velocity and density. The values obtained were $0.005<\alpha_{sh}<0.69$.

The shearing rate or dissipation parameter can be obtained from $G=\sqrt{2u_*^3 / (\upsilon h\kappa)}$, according to Nezu and Nakagawa (1993), where the von Karman coefficient κ and u_* is the shear velocity.

Floc density is an important variable and sensible changes can be observed in space and time (van Leussen, 1999). From the laboratory experiments a relationship was established among floc density, flow shear stress and suspended sediment concentration, as explained in section 3.2.

In order to consider the breakup mechanism due to shear rate, the collision frequency function K_{sh} was modified accor

$$K_{sh}\left(x,y,t\right) = G/\pi - \theta\left(\tau_b / \tau_f\right) \qquad \text{for } \tau_f < \tau_b \tag{11}$$

where τ_f, is a critical shear stress for floc breakup and θ a calibration parameter. If K_{sh} <0, then K_{sh}=0, which means the aggregation and breakup mechanisms are in equilibrium. Following Kranenburg (1994), τ_f can be written as:

$$\tau_f = \Delta\rho_f^{\frac{2}{3-n_f}} \tag{12}$$

where n_f is the fractal floc dimension. Also according to Kranenburg (1994), n_f is related to the floc diameter and the sediment particle diameter, d_p or median diameter of single particle size distribution, d_{50}, by

$$\Delta\rho_f = \Delta\rho_s \left(d_p / d_f\right)^{3-n_f} \tag{13}$$

where $\Delta\rho_s = \rho_s - \rho_w$. Flow mean velocity and depth are obtained from a depth integrated numerical mode. τ_b is calculated from the mean velocity and Manning equation, where n=0.03 as a result of the hydrodynamic calibration. Figure 1 shows the sequence of calculations in order to solve the suspended concentration field. The floc differential density $\Delta\rho_f$ was obtained from laboratory experimental data and an iterative procedure, from where the relation $\Delta\rho_f$=f(τ/C) was constructed, as can be seen in Fig. 6. In the experiments, the shears τ was computed for Couette flocculator (τ =0 and G=0 for disk flocculator were adopted) and C was measured from the experiments. For the mathematical model, τ was computed from hydrodinamic and C from the sediment transport model and $\Delta\rho_f$ was computed from the experimental relation $\Delta\rho_f$=f(τ/C).

The floc settling velocity was measured in a settling tube for the different laboratory experiments. For the mathematical model, the floc settling velocity was computed from Eq. (6) with C from the sediment transport model, and the Eq. (7) to Eq. (9). The variables ρ_w, α_b, α_{sd}, and k were adopted. The variables T, υ, G and h were computed. The parameters α_{sh} and n_f were obtained from the laboratory data.

Floc size and settling velocities were determined in laboratory, as explained in section 3.2. From this data, floc density was calculated considering the balance between submerged weight and drag (Wu and Lee, 1998):

$$\frac{\pi d_f^3}{6} g\left(\rho_f - \rho_w\right) = C_D \rho_w \frac{\pi d_f^2}{4} \frac{W_s^2}{2} \tag{14}$$

where C_D is the drag coefficient. This was calculated according to Masliyah and Polikar (1980) equations, which considers the effect of floc porosity:

$$C_D = \frac{24\Omega}{Re}\left(1 + 0.1315\, Re^{(0.82 - 0.05 \log_{10} Re)}\right) \qquad 0.1 < Re \le 7 \tag{15.a}$$

$$C_D = \frac{24\Omega}{Re}\left(1 + 0.0853\, Re^{(1.093 - 0.105 \log_{10} Re)}\right) \qquad 7 < Re \le 120 \tag{15.b}$$

where $R_e=W_s\, d_f / \nu$. Other effects, as the internal flow through the floc shown by Tsou et al. (2003) were not accounted for. Coefficient Ω is the ratio of the drag experienced by a porous floc and a solid sphere, computed from floc permeability, k_f, and floc diameter, according to Neale et al. (1973):

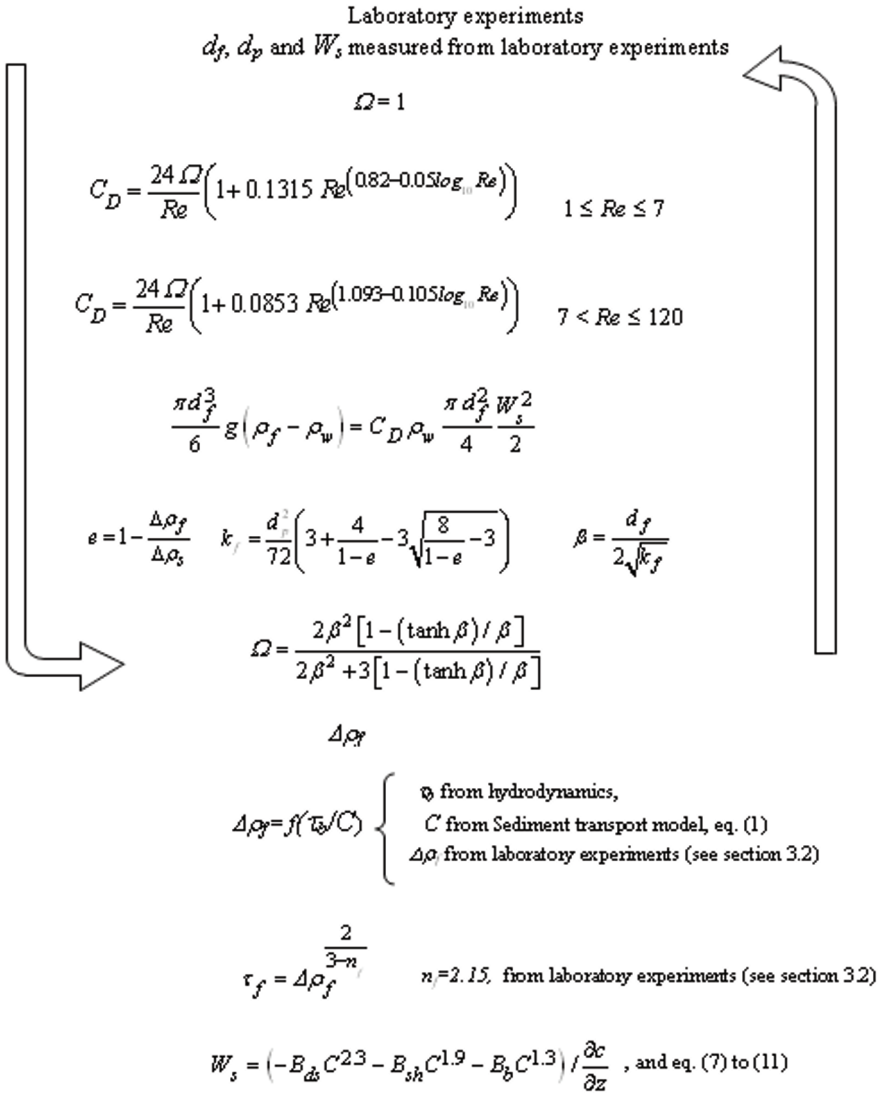

Fig. 1 Iterative procedure to compute floc differential density $\Delta\rho_f = \rho_f - \rho_w$, with ρ_f the floc density, ρ_w the water density, d_p is the median diameter of single particle size distribution, d_f is the median floc diameter, W_s is the average floc settling velocity, Ω is the ratio of the drag experienced by a porous floc and a solid sphere, e is floc porosity, k_f is floc permeability, C_D is the drag coefficient, R_e is the Reynolds number, β is dimensionless floc diameter, C is the mean concentration suspended sediment in the vertical profile, $\partial c/\partial z$ is the vertical sediment concentration gradient, τ_b is the shear stress, τ_f is critical shear stress for floc breakup, B_b, B_{ds}, B_{sh} are functional relationships representing each flocculation process and n_f is the fractal floc dimension.

$$\Omega = \frac{2\beta^2\left[1 - (\tanh\beta)/\beta\right]}{2\beta^2 + 3\left[1 - (\tanh\beta)/\beta\right]}, \quad \text{and} \quad \beta = d_f \big/ 2\sqrt{k_f} \tag{16}$$

β is dimensionless floc diameter and k_f is given by Brinkman model (Lee et al., 1996)

$$k_f = \left(d_p^2/72\right)\left(3 + 4/1 - e - 3\sqrt{8/1 - e - 3}\right) \tag{17}$$

where e is the floc porosity given by (Neale et al., 1973).

$$e = 1 - \Delta\rho_f \big/ \Delta\rho_s \tag{18}$$

We used a Newton-Raphson iterative procedure to solve Eqs. (15) to (18), with the given d_p, W_s and d_f from laboratory data, ρ_f was obtained for each measured floc, according to the scheme shown in Fig. 1. Given ρ_f, n_f is calculated from Eq. (13) and subsequently τ_f can be calculated from Eq. (12).

3 Laboratory experiments

The aim of the experiments was to measure size evolution with time and settling velocity of flocs for determining their differential density $\Delta\rho_f$, and fractal dimension n_f. Sediments from the bed and water from the estuary were sampled. Concentrations of 100, 200 and 335 mg·l^{-1} were considered representative of the natural conditions. The individual particle size was measured with a Malvern Mastersizer 2000, resulting in a d_{50}=17 μm. Clay fraction (< 2 μm) was about 10%. The salt water used in the experiments was obtained in the estuary of the Paraiba do Sul River. Mineralogy of the sediments, obtained by X ray diffraction in a Rigaku Denki – D/Max II-C instrument, showed 85% of kaolinite, 15% of illite, with muscovite, quartz and chlorites.

3.1 Experimental devices

For the laboratory experiments, two flocculators were used, as shown in Figs. 2 and 3. The disk flocculator consists of two parallel disks of transparent acrylic of a diameter of 50 cm each, separated 30 mm, and a volume of 6,500 cm^3. The flocculator was rotated by a motor (30 W), at a controlled speed. The mixture of water and sediment was poured through a lateral 10 mm diameter hole from where samples were taken at desired times (Lick et al., 1993). The sampling procedure consisted in extracting a volume of 3 cm^3 with a tube of 4 mm diameter, to avoid floc breakup. To proceed, the motor was stopped for less than 30 s.

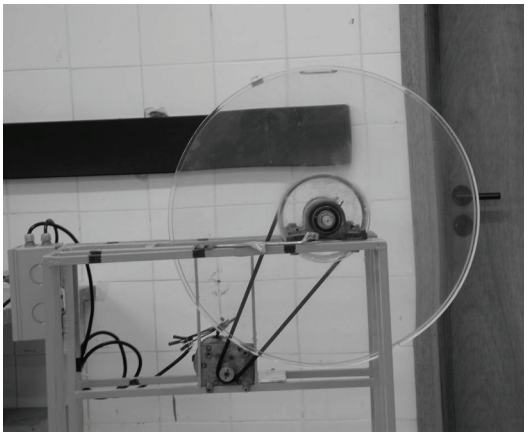

Fig. 2 Disk flocculator

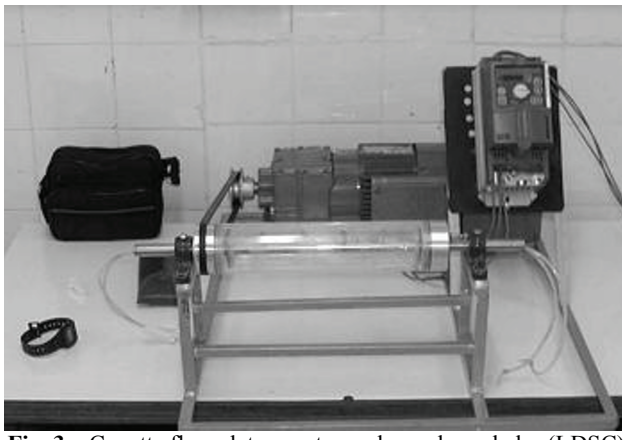

Fig. 3 Couette flocculator, motor and speed regulador (LDSC)

The disk was rotated at a constant ω = 2 rpm. The mixture inside the disk was rotated, preventing the sedimentation of flocs at the bottom. With low angular velocity flocs were formed, prevailing differential settling. Experiments were performed at pH=6.5. Table 1 shows concentration, C; salinity S; temperature, T and specific conductivity, CE for each experiment.

Table 1 Experiments in the disk iflocculator: ω is angular velocity, C is concentration, S salinity, T is water temperature and CE is the specific conductivity

ω	C	S	T	CE
rpm	mg l^{-1}	Psu	ºC	μS cm^{-1}
2	100	0.0	25.6	22.9
2	200	0.0	25.5	31.8
2	335	0.0	25.3	38.2
2	100	31.0	25.9	47,500
2	200	32.6	25.5	49,500
2	335	29.8	26.1	45,800

The Couette flocculator (Fig. 3) was built according to Tsai et al. (1987). Two coaxial horizontal cylinders were made of transparent acrylic, 25 cm long, with diameters 5.8 and 5.4 cm, for the external and internal cylinders, and a volume of 69 cm^3 in the gap. The external cylinder was rotated by a controlled motor, from 0 to 375 rpm.

Samples were taken through 3 mm hoses, located at four places distributed along the cylinder, and the volume was refilled through a hole in one of the ends. The flocculator was stopped for a short time for sampling. The conditions for the experiments are described in Table 2.

The samples taken from the flocculators were immediately studied under the microscope and photographed with a 4-megapixels Nikon Coolpix 4500 digital camera, of a 5 μm per pixel resolution. A plastic grid with 1 millimeter equidistant lines was used as a base to place the samples. Photographs were subsequently processed by proper software, thus determining the number of flocs and their characteristic size, d_f. After being photographed, the flocs were carefully placed on the upper end of a 34 cm high and 4 cm diameter transparent acrylic settling tube filled with water with the

same properties (S and T) as the flocculator. The time required for the flocs to travel a distance of 10 cm was measured by a measuring scale adhered to the tube wall. Average sedimentation velocity W_s was estimated. The tube was illuminated by a fluorescent lamp on each measurement and then darkened in order to prevent a rise in water temperature.

Table 2 Experiments in the Couette flocculator. ω is angular velocity, C is concentration, τ is shear stress, G is dissipation parameter, S is salinity, T is water temperature and CE is the specific conductivity

ω	C	τ	G	S	T	CE
rpm	mg l^{-1}	N m^{-2}	s^{-1}	psu	ºC	µS cm^{-1}
150	100	0.179	200	31.4	25.2	47,900
150	200	0.179	200	32.2	25.0	49,200
150	335	0.179	200	32.2	25.2	49,200
75	200	0.090	100	0.0	25.1	25.0

Following this procedure floc size was determined for approximately 22,000 flocs. Fresh water, salt water and estuary sediments for concentrations of 100; 200 and 335 mg·l^{-1} were used. Under shear stress conditions with the Couette flocculators 8,000 flocs were generated, and 14,000 were created with the disk flocculator. The d_f variable was measured with optic microscopy and 339 determinations of W_s were made in settling tubes.

3.2 Laboratory results

Flocs reached equilibrium when a balance between aggregation and breakup processes occurred. The d_e were obtained when mean sizes stabilize for an equilibrium time, T_e, or flocculation time (Mietta et al., 2009). In the disk flocculator, the first sample was taken after 10 minutes, and in the case of the Couette flocculator, after 5 minutes. For both flocculators it was verified that T_e was reached more quickly in salt water than in fresh water. It was observed that at lower ω greater T_e were recorded, which indicated that for the assayed stress range the collision efficiency increased with G. This result is due to the fact that greater stresses caused more collisions per time unit, forming aggregates in equilibrium more rapidly. The results obtained are shown in Tables 3 and 4, and s is the average standard deviation. For both flocculators the greater d_e corresponded to the higher C, both in fresh and salt water, in agreement with the aggregation theory and the findings of Serra and Casajmitana (1998) and Manning and Dyer (1999), among others. For the salt water samples (identified with an "S" next to the concentration), the d_e were slightly greater than those obtained from fresh water (identified with "F"). In the case of the Couette flocculator, it was observed that at lower ω, greater d_e was obtained, which indicates the limiting effect of shear stresses on the size of flocs.

Table 3 Summary of the experimental results for the disk flocculator. C is concentration, N is the number of flocs, d_e is the floc equilibrium diameter, s is the statistical deviation of the diameters and T_e is the equilibrium time for each test.

Tests with salt water				
C (mg l^{-1})	Nº Flocs	d_e (µm)	s (µm)	T_e (s)
S 100	4,023	96	52.1	1,200
S 200	4,233	125	51.5	840
S 335	2,678	145	49.2	1,620
Tests with fresh water				
C (mg l^{-1})	Nº Flocs	d_e (µm)	s (µm)	T_e (s)
F 100	651	90	66.9	1,320
F 200	1,250	95	63.8	1,440
F 335	1,087	105	60.3	1,320

Table 4 Summary of the experimental results for the Couette flocculator. C is concentration, ω is angular velocity, N is the number of flocs, d_e is the floc equilibrium diameter, s is the statistical deviation of the diameters, T_e is the equilibrium time for each test and G is the dissipation parameter

Tests with salt water (S)						
C (mg l^{-1})	ω (rpm)	Nº Flocs	d_e (µm)	s (µm)	T_e (s)	G (s^{-1})
100	150	2,181	34	18.9	420	200
200	150	534	40	23.8	510	200
335	150	1,556	44	15.4	360	200
Tests with fresh water (F)						
C (mg l^{-1})	ω (rpm)	Nº Flocs	d_e (µm)	s (µm)	T_e (s)	G (s^{-1})
100	150	450	31	19.0	420	200
200	150	866	36	18.0	660	200
200	75	1,267	45	16.0	870	100
200	38	1,372	46	21.9	600	50

The relationship between d_e and $C/G^{0.5}$ (Winterwerp, 2002), in accordance with the values in Table 4 was verified, thus obtaining a determination coefficient R^2=0.878.

Figure 4 shows the relationships d_f-W_s, with values indicating the density of flocs according to Stokes' law. In general, it can be observed that as C increases, so do d_f and W_s, while $\Delta\rho_f$ decreases. The aggregates generated with the Couette device at 150 rpm with C=100 mg·l^{-1} were the slowest and those of the highest density. For the only sample taken from the Couette flocculator with fresh water in which measuring W_s was possible, no significant differences regarding W_s of salt water were observed.

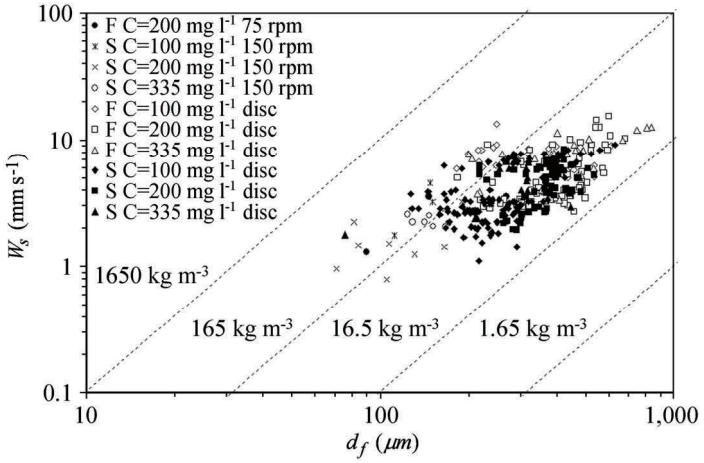

Fig. 4 Settling velocities as a function of floc diameter for fresh water and salt water. Settling velocities and diameters, as predicted by Stokes' law, for excess densities $\Delta\rho_f$ of 1.65, 16.5, 165 and 1650 kg m^{-3} are also shown

In fact, the settling velocities of two or three largest flocs of each sample were measured. Then, the average settling velocity, W_s, was computed and correlated with the flocs measured on the photos. The best results were obtained for the average 3% greater than the flocs obtained in the disk flocculator and the 4 largest flocs measured with the Couette device, in each sample.

Most flocs generated in the disk showed W_s at interval 1–10 mm s^{-1}. In general, it was possible to observe higher velocities for the flocs corresponding to higher C and lower W_s for the sample with C=100 mg·l^{-1} in salt water.

Figure 5 shows the comparison between the results obtained for C_D calculated according to Stokes' law with the adjustments due to inertial and porosity effects, evidencing significant differences for lower levels of C_D corresponding to larger floc sizes (and higher W_s, for which such effects are more important). Differences observed for $\Delta\rho_f$ considering inertial and porosity effects were 14 to 41 % for the flocs of the Couette flocculator and 1 to 59 % for those of the disk flocculator.

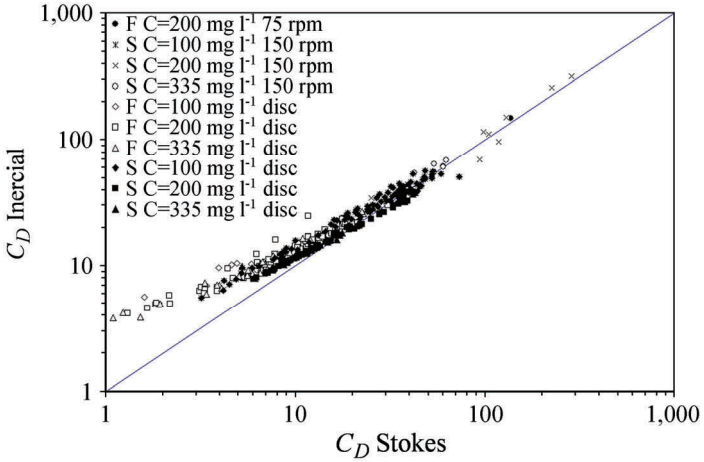

Fig. 5 Comparison of drag coefficient C_D, calculated through Stokes formula and calculated according to porosity and inertial effects with Masliyah & Polikar (1980) (Eq. 15)

Figure 6 shows the relationship obtained bewteen $\Delta\rho_f$ and the τ/C coefficient (τ=0 for the disk tests), from which $\Delta\rho_f$ was calculated in the simulations for the estuary. The adjustment equation is valid for the intervals with which it was obtained: 100< C <335 mg·l^{-1} and 0< τ <0.18 N·m^{-2}. For τ >0.18 N·m^{-2}, $\Delta\rho_f$ was adopted constant in 263 kg·m^{-3}. The

relation of $\Delta\rho_f$ as a function of τ and C shows a similar trend to that observed by Manning and Dyer (1999) in laboratory tests with sediments of the Tamar River.

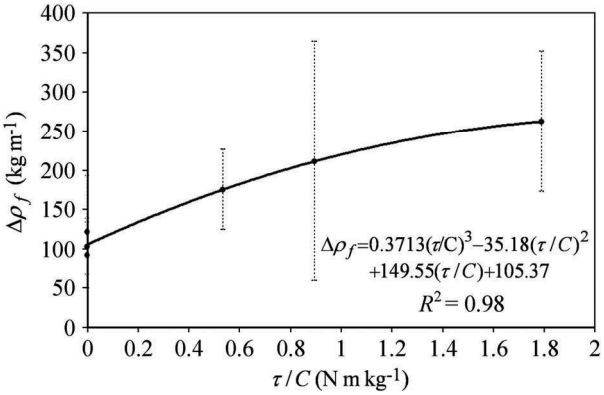

Fig. 6 Relation between $\Delta\rho_f$ and τ/C, based on laboratory experiments (deviations in vertical lines)

τ_f was obtained with Eq. (12) after calculating n_f with equation 13 by d_f and W_s measured and $\Delta\rho_f$ calculted with C_D in the non-inertial regime. Figure 7 shows the relationship between the floc breakup shear stress τ_f as a function of differential density from laboratory data, values of the fractal dimension are also indicated. The higher n_f corresponded, in general, to the samples from the disk flocculator. For the samples in salt water, W_s of 207 flocs were measured, obtaining for n_f values at interval: $1.9<n_f<2.0$, while for the samples in fresh water W_s of 132 flocs were measured, obtaining $1.8<n_f<2.1$. On average, neither group considered showed significant differences for n_f, just as they had not done so for ρ_f. Ninety per cent of the flocs whose W_s was successfully calculated in sedimentation tubes showed $1.90<n_f<2.45$, although no relevant differences were found between the flocs generated in fresh water and those generated in salt water, and using both types of flocculators.

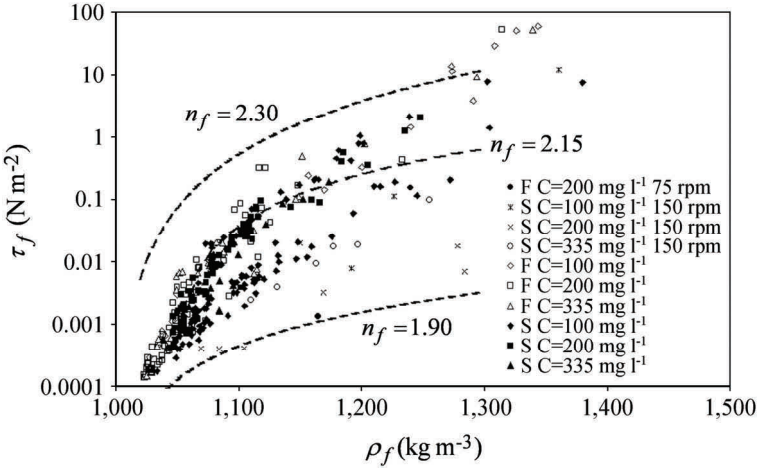

Fig. 7 Floc breakup shear stress τ_f as a function of floc density from laboratory data (fractal dimension n_f obtained from equation (13))

4 Study case: Paraiba do Sul Estuary, RJ, Brazil

4.1 Field measurements

The Paraíba do Sul River has a drainage area of 55,400 km^2, draining three of the most industrialized Brazilian states (Minas Gerais, São Paulo and Rio de Janeiro). The estuary is located at 21° 36'S, 41° 05'W, as shown in Fig. 8. A semidiurnal microtidal regime (Carvalho et al., 2002) was observed. The mouth morphology and river discharge prevent salt water intrusion, even during the dry season. The estuary has varying depths of up to 17 m. The mean flows in the rainy period range from 700 to 1,300 m^3·s^{-1}, and during the dry period they range from 400 to 500 m^3·s^{-1}. As per data provided by the Water National Agency of Brazil (ANA according to its initials in Spanish), during the period comprised between the years 1992–2002, the highest flow measured was 5,304 m^3·s^{-1} and the lowest 234 m^3·s^{-1}, with an average of 642 m^3·s^{-1}. The highest discharges occur during summer, when the river carries approximately one million tons of sediment into the sea (fine sediments mostly). Carvalho et al. (2002) suggested that these sediments may be seriously contaminated with heavy metals.

A field survey was performed in the Paraíba do Sul river estuary in January 2004, under mean river discharge conditions and neap tides. An Ndp velocity profiler was used to measure horizontal mean velocities and a probe was employed to determine turbidity, salinity, dissolved oxygen, water depth, and water temperature for 15 vertical profiles (indicated in Fig. 8). A Lisst 25X sensor was used to determine Sauter mean diameter (Smd) floc size, at 8 stations, and 27 samples of total suspended sediment concentration were obtained by means of a Wildco sampler with 2.2 l capacity. The Smd (also called d_{32} or $D[3,2]$) is used to characterize the sizes of the suspended sediment. It is defined as the diameter of a sphere that has the same volume/surface area ratio as the particle of interest. Good correlations were observed between the Smd versus d_{50} and Smd versus d_{10}, with $R^2 \sim 0.8$ and 0.9, respectively, being the d_{50} approximately 2 times higher than the *Smd* (Filippa et al., 2011). A Malvernsize laser diffraction instrument was used in the laboratory to obtain the grain size of 27 samples of the water column and 15 bed samples.

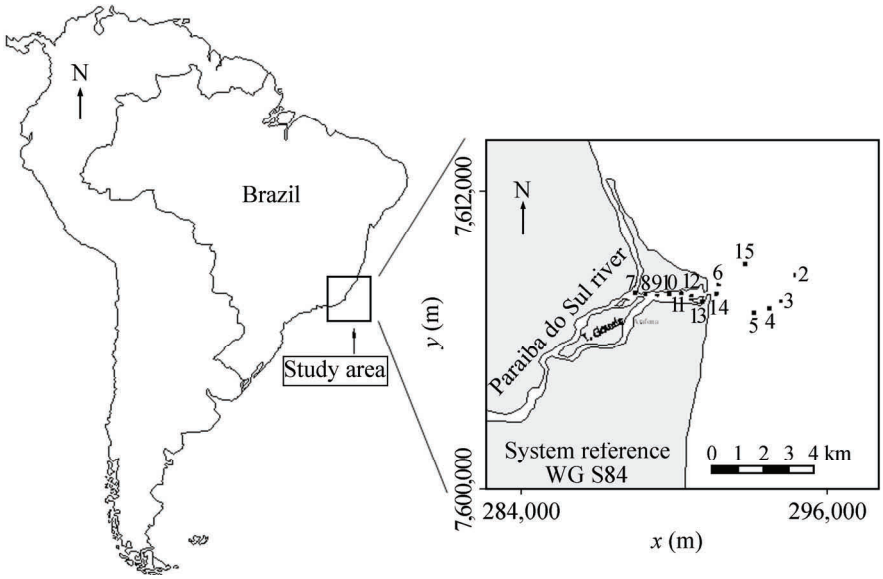

Fig. 8 Geographical location of the study reach and sampling locations. Numbers are used to indicate samples collected from the boat in vertical profiles in Paraiba do Sul estuary

4.2 Numerical modeling

The estuary hydrodynamics was simulated with a two-dimensional horizontal module of the SisBAHIA software (Rosman, 2008), vertically averaged model and solved in a finite elements mesh. The modeling domain was defined in order to cover the estuary area and adjacent shelf. The mesh consisted of 482 quadratic elements and 2229 nodes. Boundary conditions consisted of measured discharges and tidal amplitudes and phases. The bathymetry was generated from nautical charts and data collected during the survey. The hydrodynamic conditions were simulated for 10 days, corresponding to the survey, with river discharges varying from 300 to 800 $m^3 \cdot s^{-1}$. An equivalent roughness to n=0.03 was adjusted to represent the observed water levels and velocities. The sediment transport model considered $D_{xx}=D_{yy}=$ 0.36 $m^2 \cdot s^{-1}$, τ_e=0.20 $N \cdot m^{-2}$, U_{cr}=0.02 $m \cdot s^{-1}$, λ=0.85, q=0. The parameters α_{sh}=0.08 and n_f=2.15 were obtained from laboratory experiments. Sediment input into the system was simulated using a permanent vertical line and a sediment concentration of $C(0,t)$=74 $mg \cdot l^{-1}$ measured at field site.

Figure 9 and Fig. 10 show the results for the parameters of Eq. (6) for shear, $B_{sh}C^{1.9}$, and differential settling, $B_{ds}C^{2.3}$, for stations 9 and 14, located in the inner part of the estuary and on the shelf, respectively (Fig. 8). Also floc strength, τ_f, and bed shear stress, τ_b are shown for the sake of comparison. In this case the breakup mechanism was not active, as $\tau_f > \tau_b$, for most of the tidal cycle. Floc strength is related to differential density (Eq. 12) through n_f.

As it can be seen in Fig. 9 and Fig. 10, during each semidiurnal tidal cycle $B_{sh}C^{1.9} > B_{ds}C^{2.3}$ at station 9 and for an interval of 7h in 14, according to the variations of τ_b and τ_f, tending to equalize as both stresses reach their minimums. Model results demonstrated that $\tau_f > \tau_b$ during almost the whole simulation period, with the exception of an interval regarding maximum τ_b, which limited the increase in the floc size up to d_f=44 μm, for example in t=37.4 h, during 25 min (Fig. 11). When the model with n_f=2.0, 2.05 and 2.10 was executed, the intervals with $\tau_b > \tau_f$ were 6.4, 5 and 3h respectively, obtaining maximum sizes for d_f=15, 28 and 33 μm. For the growth limiter algorithm scheme of floc size of equation (11), θ=0.20 s^{-1} was employed in all the cases.

In Fig. 11, temporary variations of d_f, G, U and the height of wave z regarding the mean sea level were represented. Smd measured in situ with a Lisst 25X is also shown. As regards station 9, it can be appreciated that along the tidal cycle G presents two peaks with maximum values of 4.00 s^{-1} and 0.20 s^{-1}. The former is associated to the flow of the river into the sea, and the latter is the reverse case. Along the ascending stretch of G, floc sizes increased from $d_f \approx 25$

μm to $d_f \approx 44$ μm in $G \approx 4$. Simultaneously, U increased reaching its maximum value along with G. When G was at its maximum level the height of wave z was at a midpoint showing a descending trend and d_f fluctuated around 30 μm. Along the decreasing stretch of G, d_f decreased to 24 μm. Afterwards, floc sizes increased with the entry of sea water, which occurred at an average velocity of 0.05 m·s^{-1}. This flow proved enough for G to increase from its minimum level of 0.04 to 0.20 s^{-1}, a fact that contributed to incrementing d_f in the first place and maintaining them in $df \approx 30$ μm later. This process ceased when the flow changed into the opposite direction again, so d_f continued to grow in order to resume the same cycle. In station 9, Smd were measured at two depths: 1m and 1.8 m, obtaining sizes of 24.3 and 27.7 μm respectively (Fig. 11), adopting an average of 26 μm. The results for d_f calculated with the model agreed quantitatively with those yielded by laboratory tests with the Couette flocculator. Even when in those laboratory tests G had at least one order of magnitude larger than in the estuary, the shear stress of the flocculation (τ_b=0.179 N·m^{-2} for ω=200 rpm) remained within the same order as the calculated for the hydrodynamic conditions of the Paraíba do Sul (Fig. 9 and Fig. 10). In the interior stretch of the estuary the average τ_b stress was 0.12 N·m^{-2} for each cycle, and the maximum τ_b=0.274 N·m^{-2}.

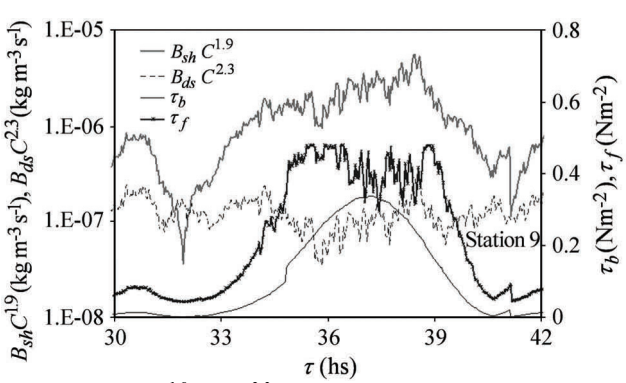

Fig. 9 $B_{sh}\,C^{1.9}$, $B_{ds}\,C^{2.3}$, τ_b and τ_f computed from model for station 9

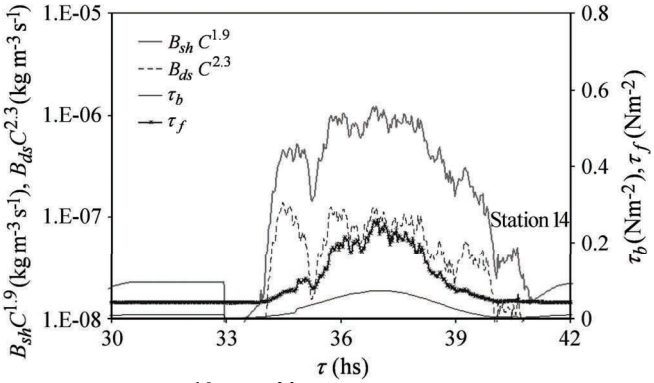

Fig. 10 $B_{sh}\,C^{1.9}$, $B_{ds}\,C^{2.3}$, τ_b and τ_f computed from model for station 14

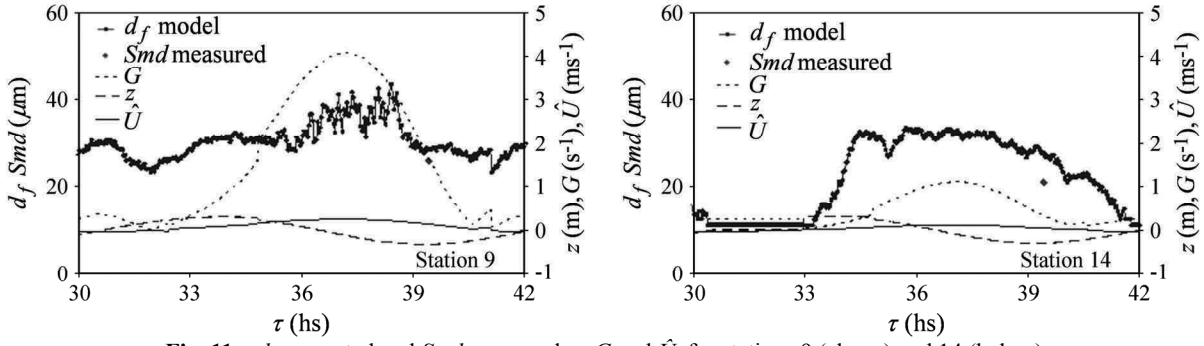

Fig. 11 d_f computed and Smd measured, z, G and $\hat{U}$, for stations 9 (above) and 14 (below)

As shown in Fig. 12 d_f values were two times larger than the d_{50} of the particles, obtained in the laboratory using a Malvern instrument: 8.4 μm<d_{50}<12 μm. It was also found that Smd, that had been measured with Lisst 25X showed a tendency to increase with the depth and the distance from the estuary mouth: 23 μm<Smd<40 μm (Fig. 12). This process agrees with the decreasing trend of G as it approaches the mouth of the estuary, thus it follows that the process of floc formation in the inner estuary is dominated by turbulent shear stress. Model results proved to be satisfactory, especially in inner estuary areas, with differences that range from 10 to 20%. C river measurements showed constant values in the vertical profiles, around 80 mg·l^{-1}, which is characteristic of well mixed waters.

In vertical 14, Smd=21 μm was measured at 2 m from the surface and d_f=28 μm was calculated for the same period, while the maximum d_f calculated was 34 μm. Aggregate sizes occurred in a context in which τ_f exceeded τb during almost the whole tidal cycle, being G and τ_b substantially lower than those in vertical 9. Nevertheless, d_f calculated in the exterior stretch of the estuary (vertical 14) were roughly 20% lower than the ones in the interior stretch (vertical 9), just like the Smd measured. These results may indicate that the aggregation process was mainly governed by C, which presented maximum concentrations with differences from 20 to 30% between both verticals.

Since it was not possible to measure settling velocities in situ during fieldwork, W_s was calculated with the Rouse formula, based on the concentration profile obtained for each water column (Fig. 13). W_s calculated at interval 0.04–0.17 mm·s^{-1} (Fig. 13) were in phase with variation of the dissipation parameter G, and of the flocs diameters d_f, a

fact that results compatible with the hypothesis of the model and the conditions of implementation. In vertical 14 concentrations decreased approximately 20% with regard to vertical 9; W_s was 0.1 mm·s^{-1} and floc sizes did not exceed 30 μm, while for $\Delta\rho_f$, 1,110<$\Delta\rho_f$<1,180 kg·m^{-3} was obtained. The differential density calculated was 1,130<$\Delta\rho_f$<1,260 kg·m^{-3} in vertical 9, with a temporary variation in phase with G. In the exterior area of the estuary 1,110<$\Delta\rho_f$<1,180 kg·m^{-3} was obtained, which corresponds to the $\Delta\rho_f$ obtained in the disk tests. Even though the $\Delta\rho_f$ calculated should not be surprising since the relationn τ/C-$\Delta\rho_f$ shown in Fig. 6 was introduced in the model, the results are consistent with laboratory results. Thus, it becomes evident that the importance of differential flocculation should not be disregarded in the exterior region of the estuary. In a numerical test with α_{ds}=0.05, $B_{sh}\ C^{1.9} \approx B_{ds}\ C^{2.3}$ relations and maximum d_f≈53 μm in both verticals considered under the same hydrodynamic conditions were obtained.

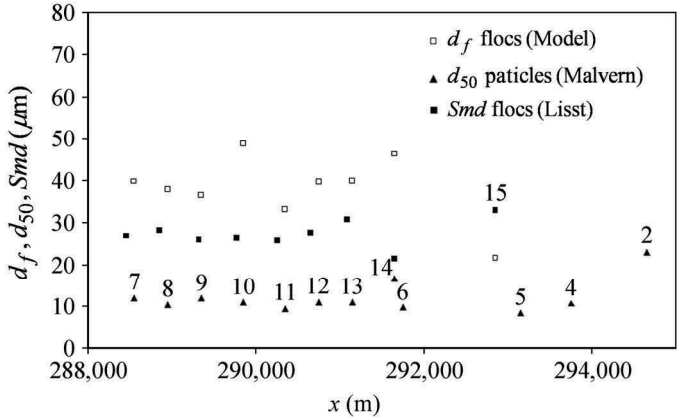

Fig. 12 d_f model, *Smd* Lisst and d_{50} (Malvern) for different stations

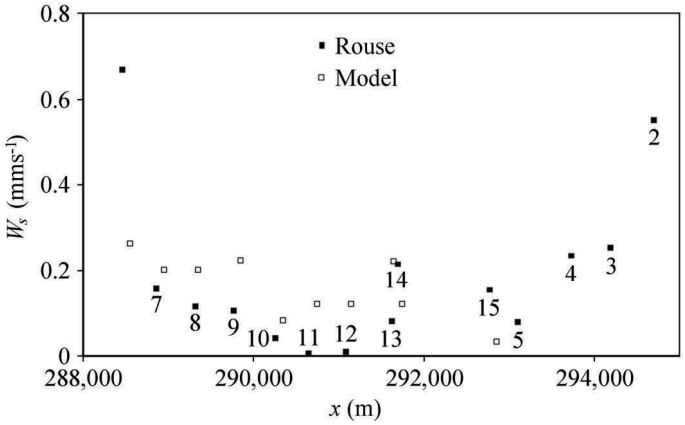

Fig. 13 W_s computed from model and Rouse equation for different stations

4 Conclusions

The characteristic size of flocs generated in two flocculators –Couette and disk flocculators– and the settling velocities of flocs in a settling tube were measured. In agreement with the aggregation theory, it was verified that floc size tends to increase as C grows. Equilibrium diameters correlate with C, both for the aggregates obtained in the disk and in the Couette flocculator. Due to the effect of shear stresses and the greater number of collisions, the flocs generated in the Couette flocculator were substantially smaller and larger density on average than the ones obtained by differential sedimentation. As C increased, size and W_s also increased, whereas ρ_f decreased. For ω=150 rpm with C=100 mg·l^{-1} the most dense and slowest aggregates were obtained. Flocs generated in the disk with salt water registered lower sizes and velocities than the ones in fresh water. In general, equilibrium diameters and W_s correlated with concentrations. All the flocs obtained in the disk with fresh water and almost all the ones in salt water registered R_e>0.50, evidencing the importance of porosity and inertial effects which were considered upon determination of drag coefficients C_D. A formula to determine the collision efficiency α_{sh} was obtained and the time scale T_e for both flocculators was calculated.

Through in situ floc measurements, a process of microflocs formation with a mean diameter of approximately three times the d_{50} size was identified to be taking place in the estuary of Paraíba do Sul River. The d_f values increased as water left the estuary, whereas G values decreased due to tidal interference. Outside the estuary area, flocculation and deposition of fine sediments were shown to be the dominant processes, favored by a decrease in turbulent shear stress which reduces the breaking up of flocs. Aggregate sizes occurred in a context in which τ_f exceeded τ_b during almost the

whole tidal cycle, with G and τ_b values higher in the interior of the estuary than those in the outer area. Thus, calculated d_f in this area were 20% smaller than the ones in interior area, in agreement with the *in situ* measured floc size. Aggregation process was also controlled by concentrations, being the maximum concentrations 20 to 30% larger in the inner area than the outer one.

Laboratory experiments proved to be helpful to obtain empirical formulas for α_{sh} and $\Delta\rho_f$, and the determination of n_f and τ_f, later used in the numerical model RWPT. In this paper an integration of laboratory flocculation experiments and numerical simulations with independent measurements of flocs at the field site was made, contributing to validating sediment transport models in a natural estuary scenario.

Acknowledgements

This work was financed by the funds granted by the CNPq (Brazil) and partially by ANPCyT, (grant PICT Nº 35885) and Universidad Nacional del Litoral (Argentina), to Dr. Afredo Trento.

References

Ariathurai R. and Arulanandan K. 1978, Erosion Rates of Cohesive Soils. Journal of Hydraulics Division, Vol. 104, pp. 279–283.

Burd A. B., Moran S. B., and Jackson G. A. 2000, A coupled adsorption-aggregation model of the POC/234Th ratio of marine particles. Deep-Sea Research Part I: Oceanographic Research Papers, Vol. 47, No. 1, pp. 103–120.

Carvalho C. E. V, Salomão M. S. M., Molisani M. M., Rezende C. E., and Lacerda L. D. 2002, Contribution of a medium-sized tropical river to the particulate heavy-metal load for the South Atlantic Ocean. Science of the Total Environment, Vol. 284, pp. 85–93.

Cheng W. P., Yu P. K., and Ruey F. Y. 2008, A novel method for on-line evaluation of floc size in coagulation process. Water Research, Vol. 42, pp. 2691–2697.

Coufort C., Bouyert D., and Linè A. 2005, Flocculation related to local hydrodynamics in a Taylor-Couette reactor in a jar. Chemical Engineering Science, Vol. 60, pp. 2179–2192.

Curran K. J., Hill P. S., and Milligan T. G. 2003, Time variation of floc properties in a settling column. Journal of Sea Research, Vol. 49, pp. 1–9.

Dimou K. N. and Adams E. E. 1993, A random-walk, particle tracking model for well-mixed estuaries and coastal waters. Estuarine, Coastal and Shelf Science, Vol. 37, pp. 99–110.

Droppo I. G., Leppard G. G., Liss S. N., and Milligan T. G. 2005, Flocculation in natural and engineered environmental systems, CRC Press, p. 438.

Edszwald J. K., Upchurch J. B., and O´Melia C. R. 1974, Coagulation in estuaries environmental. Science and Technology, Vol. 8, No. 1, pp. 58–63.

Farley K. J. and Morel F. M. 1986, Role of coagulation in the kinetics of sedimentation. Environmental Science Technology, Vol. 20, pp. 187–195.

Filippa L., Freire L., Trento A., Alvarez A., Gallo M., and Vinzón S. 2011, Laboratory evaluation of two LISST-25X using river sediments. Sedimentary Geology, Vol. 238, pp. 268-276, doi:10.1016/j.sedgeo.2011.04.017.

Friedlander S. K. 2000, Smoke, dust and haze:Fundamentals of aerosol behaviour. Wiley-Interscience.

Gibbs R. J. 1983, Effect of natural organic coatings on the coagulation of particles. Environmental Science and Technology, Vol. 17, No. 4, pp. 237–240.

Hayter E. J. and Pakala C. V. 1989, Transport of Inorganic Contaminants in Estuarial Waters. Journal of Coastal Research; Special Issue, Vol. 5, pp. 217–230.

Huang H. 1994, Fractal properties of flocs formed by shear and differential settling. Physical Fluids, Vol. 6, No. 10, pp. 3229–3236.

Hunt J. R. 1982, Self-similar particle-size distributions during coagulation: Theory and experimental verification. Journal of Fluids Mechanics,Vol. 122, pp. 169–185.

Ives K. J. and Bhole A. G. 1977, Study of flowthrough couette flocculators - II. Laboratories studies of flocculation kinetics. Water Research, Vol. 11, pp. 209–215.

Ives K. J. and Bhole A. G. 1973, Theory of flocculation for continuous flow system. Journal of the Environmental Engineering, Vol. 99, pp. 7–34.

Jackson G. A. 1994, Particle trajectories in a rotating cylinder: Implications for aggregation incubations. Deep Sea Research, Vol. 41, pp. 429–437.

Jin X.Y., 1993, Quasi Three-Dimensional Numerical Modelling of Flow and Dispersion in Shallow Water, Ph D Thesis, Department of Civil Engineering, Delft Univ. of Technology.

Johansen C. and Larsen T. 1998, Measurement of settling velocity of fine sediment using a recirculated settling column. Journal of Coastal Research, Vol. 14, No. 1, pp. 132–139.

Kim A. S. and Stolzenbach K. D. 2004, Aggregate formation and collision efficiency in differential settling. Journal of Colloid and Interface Science, Vol. 271, No. 1, pp. 110–119.

Kranenburg C. 1994, The fractal structure of cohesive sediment aggregates. Estuarine, Coastal and Shelf Science, Vol. 39, pp. 451–460.

Kumar R. G., Strom K. B., and Keyvani A. 2010, Floc properties and settling velocity of San Jacinto estuary mud under variable shear and salinity conditions. Continental Shelf Research, Vol. 30, pp. 2067–2081.

Lau Y. L. and Krishnappan B. G. 1992, Size distribution and settling velocity of cohesive sediments during settling. Journal of Hydraulic Research, Vol. 30, No. 5, pp. 673–684.

Lee D. J., Chen G. W., Liao Y. C., and Hsieh C. C. 1996, On the free-settling test for estimating activated sludge floc density. Water Research, Vol. 30, No. 3, pp. 541–550.

Lick W., Huang H., and Jepsen R. 1993, Flocculation of fine-grained sediments due to differential settling. Journal of Geophysical Research, Vol. 98, No. 6, pp. 10279–10288.
Logan B. and Kilps J. R. 1995, Fractal dimensions of aggregates formed in different fluid mechanical environments. Water Research, Vol. 29, No. 2, pp. 443–453.
Mcanally W. H. and Mehta, A. J. 2002, Significance of aggregation of fine sediment particles in their deposition. Estuarine, Coastal and Shelf Science, Vol. 54, pp. 643–653.
Manning A. J., Friend P., Prowse N., and Amos C. 2007, Estuarine mud flocculation properties determined using an annular mini-flume and the LabSFLOC system. Continental Shelf Research, Vol. 27, pp. 1070–1085.
Manning A. J. and Dyer K. R. 1999, A laboratory examination of floc characteristics with regard to turbulent shearing. Marine Geology, Vol. 160, No. 1–2, pp. 147–170.
Masliyah J. H. and Polikar M. 1980, Terminal velocities of porous spheres. Canadian Journal Chemical Engineering, Vol. 58, pp. 299–302.
Mehta A. J. and Partheniades E. 1975, An investigation of the depositional properties of flocculated fine sediments. Journal of Hydraulic Research, Vol. 13, No. 4, pp. 361–381.
Mietta F., Chassagne C., and Winterwerp J. 2009, Shear-induced flocculation of a suspension of kaolinite as function of pH and salt concentration. Journal of Colloid and Interfase Science, Vol. 336, pp. 134–141.
Mikes D., Verney R., Lafite R., and Belorgey M. 2004, Controlling factors in estuarine flocculation processes experimental results with material from the Seine Estuary, Northwestern France. Journal Coastal Research, Vol. Special Issue 41.
Milligan T. G. and Hill P. S. 1998, A laboratory assessment of the relative importance of turbulence, particle composition, and concentration in limiting maximal floc size and settling behaviour. Journal Sea Research, Vol. 39, pp. 227–241.
Neale G., Epstein N., and Nader W. 1973, Creeping flow relative to permeable spheres. Chemical Engineering Science, Vol. 28, pp. 1865–1874.
Neumann L. E. 2004, Modelling of flocculation and settling of suspended sediments using Population Balances, Ph.D. Thesis, University of Queensland.
Nezu I. and Nakagawa H. 1993, Turbulence in open-channel flows, International Association for Hydraulic Research, Monograph Series, Balkema, Rotterdam.
Nicholas A. P., Walling D. E., Sweet R. J., and Fang X. 2006 New strategies for upscaling high-resolution flow and overb ank sedimentation models to quantify floodplain sediment storage at the catchment scale. Journal of Hydrology, Vol. 329, pp. 577–594.
Rosman P. 2008, Referência Técnica do SisBaHiA®, (http://www.sisbahia.coppe.ufrj.br).
Serra T., Colomer J., and Logan B. 2008, Efficiency of different shear devices on flocculation. Water Research, Vol. 42, pp. 1113–1121.
Serra T. and Casamitjana X. 1998 Effect of the shear and volume fraction on the aggregation and breakup of particles. AIChE Journal, Vol. 44, No. 8, pp. 1724–1730.
Tooby D. T., Wicks G. L., and Isaacs J. D. 1977, The motion of a small sphere in a rotating velocity field: A possible mechanism for suspending particles in turbulence. Journal of Geophysical Research, Vol. 82, pp. 2096–2100.
Torfs H., Mitchener H., Huysentruyt H., and Toorman E. 1996, Settling and consolidation of mud/sand mixtures. Coastal Engineering, Vol. 29, pp. 27–45.
Tsai C. H., Iacobellis S., and Lick W. 1987, Flocculation of fine-grained lake sediments due to a uniform shear stress. Journal of Great Lakes Research, 13, No. 2, pp. 135–146.
Tsou G. W., Wu R. M., Yen P. S., and Lee D. J. 2003, Advection flow through sludge flocs. Advances in Environmental Research, Vol. 7, pp. 733–737.
van Duuren A. 1968, Defined velocity gradient model flocculator. Journal of the Sanitary Engineering Division, Vol. 94, pp. 671–682.
van Leussen W. 1999, The variability of settling velocities of suspended fine-grained sediment in the Sem estuary. Journal Sea Research, Vol. 41, pp. 109–118.
Walker H. W. and Bob M. M. 2001, Stability of particle flocs upon addition of natural organic matter under quiescent conditions. Water Research, Vol. 35, No. 4, pp. 875–882.
Winterwerp J. 2002, On the flocculation and settling velocity of estuarine mud. Continental Shelf Research, Vol. 22, pp. 1339–1360.
Wu R.M. and Lee D.J. 1998, Hydrodynamic drag force exerted on a moving floc and its implication to free-settling tests. Water Research, Vol. 32, No. 3, pp. 760–768.
Yang Z., Baptista, A. and Darland J. 2000, Numerical modeling of flow characteristics in a rotating annular flume. Dynamics of Atmospheres and Oceans, Vol. 31, pp. 271–294.